---

**Article:**
Ogundiran, Y., Griffo, A. orcid.org/0000-0001-5642-2921, Sundeep, S. et al. (1 more author) (2022) A novel embedded sensor for partial discharge detection in inverter-fed machines. IEEE Transactions on Industry Applications, 58 (4). pp. 4698-4707. ISSN 1939-9367

https://doi.org/10.1109/TIA.2022.3177172

---

# A Novel Embedded Sensor for Partial Discharge Detection in Inverter-fed Machines

Yinka Leo Ogundiran, Graduate *Student Member, IEEE*, Antonio Griffo, Member, IEEE, Shubham Sundeep, Graduate Student Member, IEEE, and Jiabin Wang, Senior *Member, IEEE*

***Abstract*—This paper presents a novel ring-shaped hybrid fractal antenna for detection of partial discharge (PD) in inverter-fed machines. Partial discharge is known as a source of degradation and lifetime reduction in the machines winding insulation. PD activity is becoming a major concern in high performance drives, especially due to the increased use of repetitive impulse voltage with short rise-time (high dv/dt) from PWM-controlled inverters. The proposed hybrid fractal antenna is designed and experimentally demonstrated to show a high sensitivity in the ultra-high frequency (UHF) bandwidth of interest for PD detection as well as an ability to discriminate PD signals from other sources of high frequency disturbances. Additionally, the proposed PD sensing solution features a unique ring-shape geometry which facilitates its physical integration to a live machine, making it suitable as a non-invasive solution for online condition monitoring and PD detection of any inverter-fed electrical machine.**

***Index Terms*— Electrical machine insulation, end-winding, hybrid Hilbert fractal antenna, partial discharge (PD)**

## I. INTRODUCTION

THE use of inverter-fed electrical drives is becoming widespread in systems where the requirements for reliability and availability are paramount, such as aerospace applications, electric vehicles and ship propulsion [1]–[3]. The requirements for high efficiency and power density in these applications is driving a trend to use higher voltages and faster switching wide-band gap (WBG) based devices, such as those based on silicon-carbide (SiC) and gallium nitride (GaN) that yield voltage rise-times in the region of a few and few tens of nanoseconds [4]–[8]. DC link voltages of 800 V and higher are becoming common in the newest generations of electric vehicles and 1500 V is being proposed in the latest 'more electric aircrafts' (MEA) power systems design. Unfortunately, the use of pulse-width modulated (PWM) converters, especially in combination with higher voltages and faster switching transients, may produce excessive voltage stress on machine insulation which is detrimental to their lifetime.

Wave propagation and reflection across the cables and machines excited by fast-switching devices can result in excessive voltage and non-uniform voltage distribution across the machine windings and the insulation [2]. The problem is particularly critical with fast WBG devices with slew rate ($dv/dt$) in excess of 10 kV/$\mu s$ resulting in significant transient over-voltages at the motor terminals and across the machine insulation which can exceed twice of the dc-link voltage[9], [10] . Overvoltages can induce partial discharge (PD) events when the voltage level across the insulation exceeds the PD inception voltage (PDIV). For medium-voltage (>1 kVrms) and high-voltage machines categorised as Type II machines by IEC [11] which use inorganic epoxy mica stator winding insulation, PD is common and may be permitted to a certain degree. But for low voltage machines, known as Type I machines (rated voltage ≤ 700 Vrms and generally random wound) [12], the consequence of PD is particularly damaging as their thin organic insulation layers are likely to puncture as a result of PD [13]. Any occurrence of PD on Type I machines can escalate rapidly, leading to permanent damage to the insulation, and, ultimately, a complete machine failure [2], [14]–[16]. It has been recently demonstrated that the combination of short rise-time and high switching frequencies can result in overvoltages exceeding the PDIV [17], [18]. Since PD events initiated by impulsive waveforms from PWM have detrimental effect on the organic materials of random-wound insulation, PD monitoring is essential in high reliability applications [19]. It is therefore of great industrial interest to develop reliable and non-invasive PD detection sensors and methods for online condition monitoring of inverter-fed machines [20], [21]. Studies have shown that an embedded sensor at the time of manufacturing is beneficial as it enables periodic online tests and proper scheduling of replacement for machines affected by PD [13], [15], [22].

Several PD monitoring solutions are available in grid-connected (50-60 Hz) transformers, switchgears, substations and electrical machines with different voltage levels. The most widespread PD monitoring systems use sensors based on high-bandwidth current transducers, Rogowski coils, coupling capacitors, optical and antenna-based solutions. However, the effectiveness of these systems for PD detection in inverter-fed machines is hindered by a number of factors such as impulsive voltages as a result of high *dv/dt*, presence of significant noise emanating from the commutation of PWM converters which obscures PD signals, the existence of simultaneous PD sources and the shielding effect of machines' cases which make the use of external sensors problematic [25].

The high bandwidth requirements for PD sensors in applications with PWM voltages make antenna-based solutions particularly attractive. A number of antennas have been proposed to detect PD in inverter-fed drives in the literature. PD tests under impulsive voltages were conducted using an electric monopole with centre band of 1GHz in [23]. A non-intrusive sensor, realized with the combination of a stripped coaxial cable connected to SMA (Sub-Miniature version A) jack and high-pass filter, was proposed in [24]. Other sensor types that have been applied to PD monitoring systems include the Archimedes spiral antennas [25]–[27], Hilbert antenna [28], [29], Vivaldi antenna [30], Patch antenna [31]–[33], optical sensors[34]–[36], etc. However, apart from these sensors not being originally designed for PD detection, they all have geometrical constraints which make them infeasible for physical integration to a machine in service for online PD detection, and therefore

cannot be used as embedded sensors in a machine. And the sensors employed are sometimes installed at the terminals of the machine to detect the current pulses created by PD events [37]–[40]. Unfortunately, the measurement of PD pulses with such method has inherent limitation: the signals detected by the sensors are contaminated by the aforementioned noise from WBG commutation which overlaps with frequency spectra of PD pulses and thereby inhibits the effectiveness of the detection[41]. Additionally, the PD signal, propagated as an electromagnetic wave in the insulation cavities, is affected by inverse square law which causes the signal strength to attenuate rapidly with increasing distance of the sensors from the discharge site, which often results into a poor signal-to-noise ratio (SNR). This problem always necessitates the application of external high-pass filters to reject the noise or some non-trivial signal processing technique to discriminate between the noise and the PD signals, which can be computationally expensive.

In view of the geometrical constraint of machine winding insulation and the associated problem of noise, an effective sensor that can be installed inside a machine in service with minimum invasiveness and less sensitivity to noise has not been found in the literature. This work will propose a new concept for PD detection based on a Hilbert fractal antenna specifically designed for integration with electrical machines. The benefits of integration, as well as its performances, are illustrated in this paper.

The rest of the paper is organized as follows: Section II describes the challenges associated with PD detection in inverter-fed machines and how the proposed embedded sensor addresses these challenges. Section III presents the validation of the proposed sensor with PD experimental results from a PD surge generator and an inverter-fed machine in service. Finally, Section IV concludes the paper.

## II. PD Detection

### A. *PD signals in Inverter-fed Machines*

To design sensors for PD monitoring in inverter-fed electrical machine, it is essential to understand the signal type, its spectral characteristics, and to ascertain (1) the bandwidth which the PD signal will occupy, (2) the radiation pattern which will characterize the directivity of the antenna, and (3) the scattering parameters (i.e. the reflection coefficient $S_{11}$) [42]. An effective sensor for PD detection under impulsive voltage should have ultra-wide bandwidth with a frequency spectrum that spans, at least, from 0.5 GHz to 2 GHz. Considering that the switching events in WBG devices have spectral contents that spread in the tens of MHz, which impairs the ability to discriminate PD signals from commutation noise, a detection system should incorporate high pass filter that rejects the switching noise.

By way of example, Fig. 1 shows the signal captured by a UHF antenna following a PD event in a motor fed by a SiC converter at 20 kHz PWM switching frequency, 60 ns rise time, and 800 V DC link voltage. The filtered signal through a 500 MHz high pass filter is also shown. From the spectral visualization of the signals as shown in Fig. 2, it is evident that the PD signal has a significant spectral content in the range >400 MHz - 1.5 GHz as well as the need for band-pass filtering

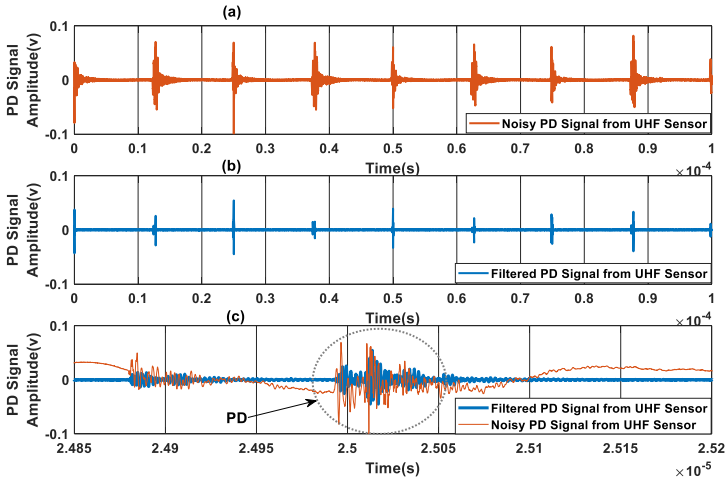


Fig. 1. Unfiltered PD signal (top) filtered PD signal (middle) and zoomed superimposition of both(bottom) from a UHF antenna illustrating how the commutation noise obscures PD signals.

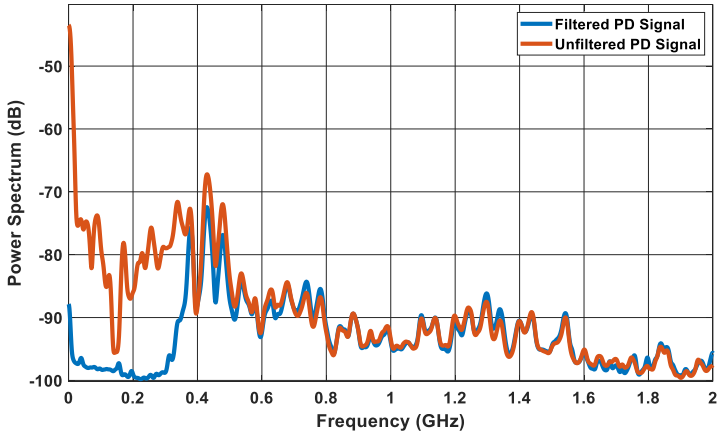


Fig. 2. Frequency domain of filtered and unfiltered signal.

to isolate the signal of interest from the background noise due to switching.

As most of the sensors reported in the literature are general purpose antennas which were not specifically designed for PD detection, they are inadequate for sensing the PD signals in the electromagnetic field that is radiated in the insulation systems of electrical machines fed by fast switching inverters. Besides the limitations of their electromagnetic characteristics, their physical design might also hinder their integration in an online electric machine monitoring system. Machines are expected to be exposed to sustained vibration and harsh operating conditions. Their sensors therefore ought to be embedded without any mechanical infringement to the rotor and stator[1]. Since the sensitivity of a sensor to detect PD depends on its proximity to the site of PD events [32], [40], it would be beneficial to install the sensor in the near field to enable it act as a capacitive coupler to the windings[43]. There are two main benefits of installing a sensor in the near field region. First, there is a greater intensity of electromagnetic power in the near field which implies a higher signal-to-noise ratio (SNR) of the PD signal. Second, there is less likelihood of interference from external sources which could potentially obscure PD signal from being detected. Using the geometry of a permanent magnet synchronous machine (PMSM) as an example, considering that the windings in slots are arranged in a circular configuration, the geometry of the PD sensor should align with

the configuration of the slot to obtain maximum directivity. The thickness of the sensor structure needs to be carefully chosen to ensure that it can be easily retrofitted close to the end-windings, and it is not obstructing the motor frame which could also provide a shielding effect by acting as a Faraday cage against interference.

The only sensor that simultaneously meets all these criteria in the literature was first proposed by the authors in [1]. The sensor, a ring-shaped structure made of a hybrid of Hilbert fractal curves, exhibits an ultra-wide bandwidth, and can easily be retrofitted to the end-winding of an electrical machine. The effectiveness of this hybrid Hilbert fractal antenna (HHFA) has however neither been physically integrated nor proven on a machine fed by a PWM-driven inverter operating at high *dv/dt* and short risetime. This paper provides a more detailed analysis of the concept proposed in [1] while also physically integrating the sensor to the end-winding of a machine and demonstrating its performances in realistic operating conditions.

### *B. PD Sensors, Design and Simulation*

To detect PDs with high sensitivity in a noisy electromagnetic environment, this work presents a novel low-cost sensor primarily conceived to be retrofitted in the end-winding of a random wound electrical machines. It exhibits wide bandwidth that covers the typical frequency spectrum of PD in PWM-controlled inverter-fed drives, yet less sensitive to electromagnetic interference from WBG devices switching in the so-called "blind region" where PD detection is considered impossible [44], [45]. The proposed sensor is based on a Hilbert fractal curve, which was re-engineered into a hybrid antenna. The sensor features a dual 36-element fractal structures which form a dipole. Its ring-shape geometry encircles the machine end-winding to have directivity to detect PD signal in all directions, as well as avoid mechanical contact with the rotor during drive operation. The simulations and analyses of the proposed sensor are performed using CST Microwave Studio suite.

A 3D illustration of the proposed concept of physically integrating a sensor close to the end winding of an electrical machine is presented in Fig. 3 while the structure of the sensor is depicted Fig. 4. The sensor is designed on a low-cost FR4 substrate with $\varepsilon_r$= 4.4, and tan$\delta$ = 0.02 and thickness = 1.5 mm. The substrate ring-shape dimensions are as follows: Outer diameter: 118 mm, Inner diameter: 80 mm, For the hybrid Hilbert fractal elements, the diameter of the inner element is 95.25 mm while that of the outer element is 100 mm, respectively. The structure consists of dual 36-element of Hilbert fractal curves which are geometrically spaced apart by 10 degrees, with the dual 36-element structures configured to form a dipole. The feedline is on the topside while there is a copper-fill on the backside, which acts as a reflection plane to improve the radiation captured by the sensing elements.

The rationale for choosing a fractal-based structure for the proposed sensor is explained in the following. Consider that the theoretical fundamental limit of an electrically small antenna is governed by Chu limit which states that the Q-factor is proportional to the reciprocal of the volume of a sphere in which it is enclosed. This is expressed as [46], [47]:

$$Q = \frac{1}{k^3a^3} + \frac{1}{ka} \approx \frac{1}{k^3a^3} \quad (1)$$

where $k = \frac{2\pi}{\lambda}$ is the wavenumber and $a$ is the sphere radius that encloses the volume. The bandwidth of an antenna is related to the Q by[48]:

$$\frac{\Delta f}{f_0} = \frac{1}{Q} \quad (2)$$

where $f_0$ is center frequency and $\Delta f$ is the bandwidth. From the above, it is implied that the bandwidth of an antenna is determined by its utilization of available volume within a structure, characteristic length and geometrical configuration [48]. Given the cylindrical geometry of an electrical machine, it is extremely difficult to design a non-invasive sensor with an ultra-wide bandwidth which PD signal spectrum usually occupies with a typical Euclidean antenna. But, with fractals, it is possible to efficiently utilize the available space in the end-winding region of a machine insulation geometry based on these two main reasons: 1) Fractals have no characteristic size and their bandwidth, therefore, are not constrained as in the case of Euclidean-based antennas. 2.) Fractals have irregular shapes which can be fitted into any geometry [49]. Also, the sharp shapes, sudden bends and discontinuities of fractal antennas contribute to the enhancement of their radiation and sensitivity [48]. Additionally, a fractal antenna can be easily printed on a rigid or flexible printed circuit board (PCB) and, thus, can be very suited to the intended physical integration in a machine.

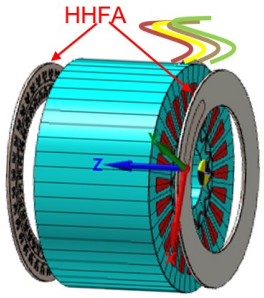


Fig. 3. Concept of PD sensor integration in the end cap of an electric machine.

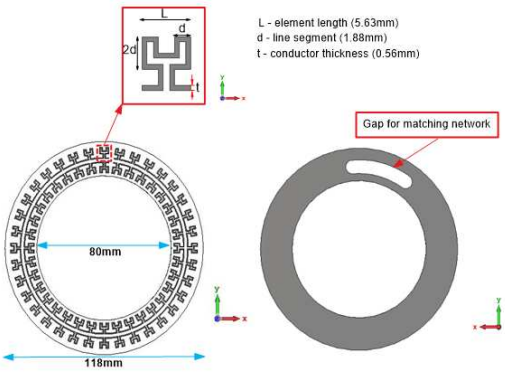


Fig. 4. Geometry of the proposed Fractal sensor (left) and reflection plane (right) [1].

The specifications on the bandwidth can be translated to a reflection coefficient lower than -10 dB, which is equivalent to voltage standing wave ratio (VSWR) of less than 2.0, in a suitable range of frequencies. The multi-resonant frequencies spans across the UHF spectrum (0.3-3 GHz), as demonstrated by the calculated reflection coefficient $S_{11}$ and radiation patterns

shown in Fig. 5 and Fig.6, respectively. Differently from a Euclidean antenna, the fractal design results in a large number of resonance peaks, potentially improving the ability to detect wide bandwidth signal such as PD.

The structure was simulated with the Frequency Domain Solver of CST Microwave Studio, which is based on the finite element method (FEM). It transforms Maxwell's equations into frequency domain by assuming time-harmonic dependence of the fields and the excitation. The discretization of the geometry was performed using tetrahedral meshing which is automatically generated by CST Microwave Studio[1].

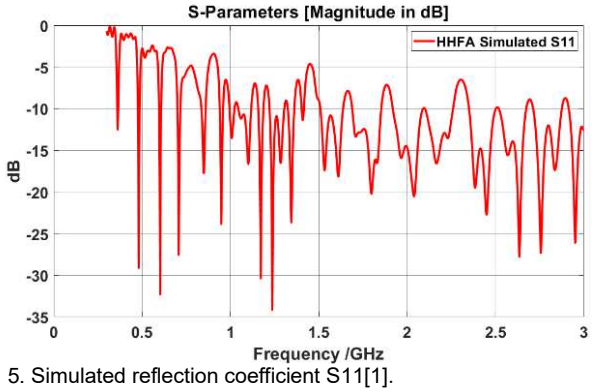


Fig. 5. Simulated reflection coefficient S11[1].

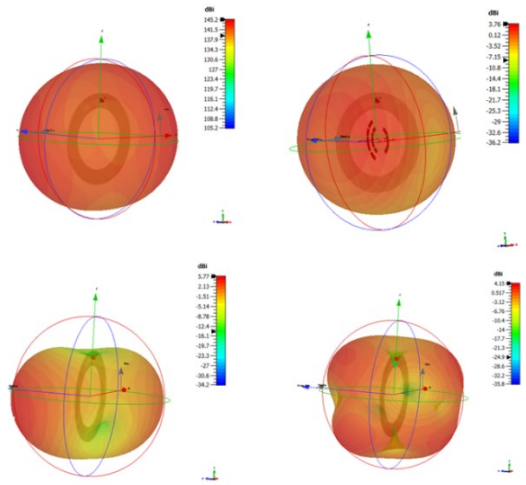

Fig. 6: Radiation pattern of the proposed sensor at 0.5 GHz (top left), 1 GHz (top right), 1.5 GHz(bottom left) and 2 GHz(bottom right) respectively.

### C. *Matching Network*

To minimize reflection and maximize power transfer between the HHFA and a receiver for monitoring PD event, an impedance matching network is required. In addition to their perimeter length and space filling characteristics, the fractals require high input impedance to obtain a large bandwidth. The HHFA was designed and optimized with 200 Ω reference impedance which would result into a mismatch and cause a reflection when connected to a 50 Ω coaxial cable used by oscilloscope and other signal processing devices. A matching network was accordingly conceived to interface the HHFA with a 50 Ω coaxial cable. There are various methods for designing an impedance network which include Smith chart, analytic solutions, single- or double-stub tuning, quarter-wave transformer, T and π-networks and others which can be found in [48], [50], [51]. The Smith Chart is the simplest method for designing a matching network as it enables a geometrical visualization of the load relative to the reflection coefficient, but its computational accuracy is low as it involves visual interpolation between the chart grid circles. It is therefore impracticable for a multi-resonant ultra-wide bandwidth sensor like HHFA. Another widespread method to implement impedance matching network is the use of a lumped element L-section to match a load to a source with two reactive elements (inductors and capacitors). However, there are only two possible configurations for a simple L-section network which

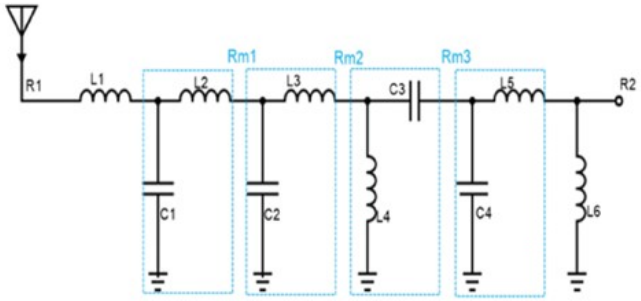


Fig. 7. 4-section interstage impedance matching network.showing connection between HHFA(R1) and coaxial cable(R2) Design parameters: L1=5.6 nH, C1=0.3 pF, L2=22 nH, C2=0.7 pF, L3=22 nH, L4=33 nH, C3=2.7 pF, C4=1.8pF, L5=8.2 nH, L6=68 nH [1]

constrains its applicability. Moreover, it is not feasible for frequencies up to 1 GHz [50], [51]. Given that the HHFA is ultra-wide bandwidth antenna, a simple L-section will be inadequate. This limitation can however be overcome and its bandwidth extended beyond 1GHz by cascading it to form an interstage network topology[52]. A 4-stage cascade of lumped element L-section with reactance cancellation which makes the impedance purely resistive (Z ≈ R) was thus designed to match the 50 Ω impedance as shown in Fig. 7.

Each of the LC sections was designed to match its impedance to the next section. The C1-L2 matches R1 = 200 Ω from HHFA to Rm1, the C2- L3 matches Rm1 to Rm2, the L4-C3 matches Rm2 to Rm3, and C4-L5 matches Rm3 to R2=50 Ω. Both L1 and L6 are used for improving the bandwidth. The relationship between the sections is given by:

$$\frac{R_1}{R_{m1}} = \frac{R_{m1}}{R_{m2}} = \frac{R_{m2}}{R_{m3}} \tag{6}$$

The bandwidth of the lumped element matching network is related to $R_{m3}$ and $R_2$ by the following:

$$Q_L = \sqrt{\frac{R_{m3}}{R_2} - 1} \tag{8}$$

The value of $Q_L$ was calculated and optimized using AWR Microwave Software to obtain an ultra-wide bandwidth (~2 GHz) that covers the expected spectrum of PD in inverter-fed Type I machines. The design parameters are shown in Fig. 7.

## III. Experiments and Results

### A. *Verification of the Sensor*

The measurement of a fabricated prototype of HHFA, shown in Fig. 8, was performed with a Siglent SVA1015X vector network analyzer (VNA) with 9 kHz - 1.5 GHz bandwidth. The measurement result of the reflection coefficient <-10 dB is in agreement with simulation, and it confirms the presence of

multiple resonances in the region of interest between 0.3-1.5 GHz as depicted in Fig. 9.

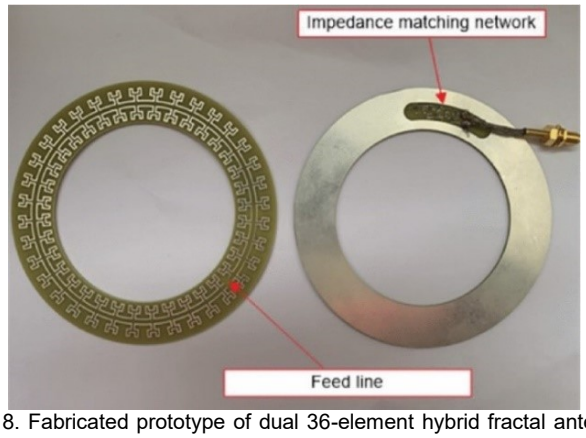


Fig. 8. Fabricated prototype of dual 36-element hybrid fractal antenna (left) and the back reflection plane (right) [1].

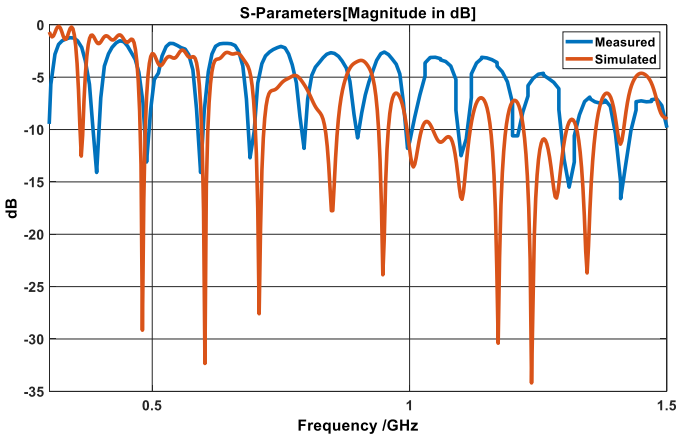


Fig. 9. Measured and simulated reflection coefficient of HHFA

Additionally, as has been discussed, one of the objectives of this work was to develop a novel sensor for online PD detection with inherent ability to discriminate PD pulses from switching and background noises in the blind region. Fig. 10 compares the output signals from HHFA and a commercial PD sensor which were obtained at 40 kHz PWM switching frequency with applied voltage < the PDIV of the given machine sample. Clearly, the HHFA, with its interstage impedance matching network, captures less switching noise, compared with that by commercial PD sensor shown at the bottom in Fig. 10, whose frequencies overlap with those of PD pulses. This implies that a commercial antenna requires an external filter before it can be used for PD detection. This demonstrates the suitability of the HHFA for PD detection in a noisy environment without the need for external filter.

### *B. PD Testing Under Surge Generator*

To assess the feasibility of physically integrating a sensor to the end-winding of a machine, the prototype shown in Fig. 8 was employed in a bespoke test rig constructed for experimental validation as shown in Fig. 11. This experiment was carried out to simulate the effect of physically embedding a sensor in close proximity to the site of PD events. For this purpose, a commercial voltage pulse generator (6 kV Schleich MTC2 multipurpose winding analyzer) with adjustable voltage level was employed to generate high voltages resulting in PD pulses across a twisted pair wire. The twisted pair, made of enamel wires, was inserted inside one of the slots of a laminated stator core and connected to surge clamps. The HHFA, which was embedded to the back of the stator, together with the laminated stator and surge clamps were placed inside an enclosure as can be seen from Fig. 12b. The off-the-shelf winding analyzer antenna (WAA) for PD detection with MTC2 was placed outside of the enclosure to monitor the PD events and provide a comparison of their performance.

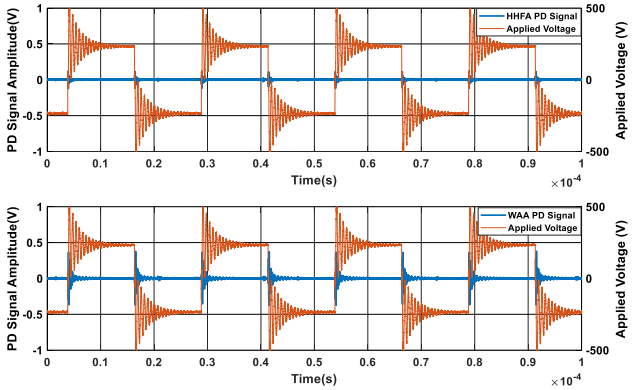


Fig. 10. Comparison of HHFA (top) and commercial sensor(bottom) in detection of electromagnetic waves propagation in a machine sample

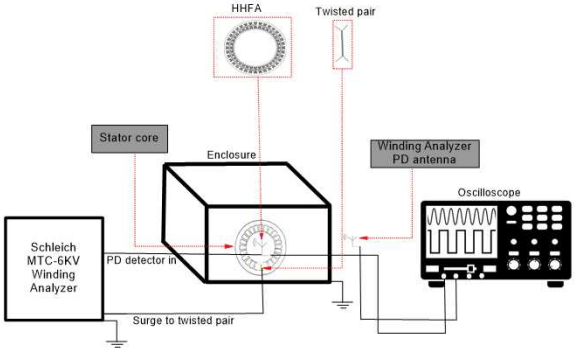


Fig. 11. PD monitoring experimental set-up. [1].

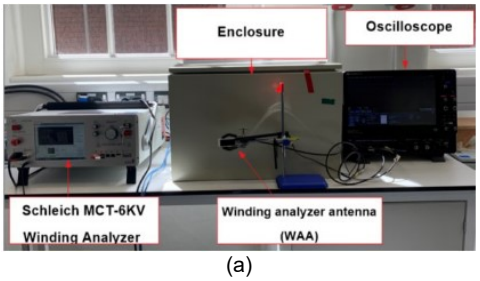


(a)

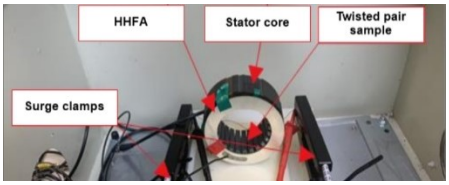


(b)

Fig. 12. Arrangement of equipment for experiment: (a) Setup showing pulse generator and enclosure, (b) Integration of HHFA to end-winding inside enclosure [1].

The PD signal outputs from both the HHFA and WAA were connected to Teledyne Lecroy WavePro 404HD-MS oscilloscope with 4 GHz bandwidth and 10 GS/s sampling rate.

A differential probe was used to record the voltage across the twisted pair. The experiments were carried out at room temperature and pressure. The PD events were triggered by application of voltage pulses generated by MTC2 across the twisted pair higher than its PDIV, and the electromagnetic signals were obtained with both HHFA and WAA. In the first experiment, a 500 MHz high pass filter was connected to both HHFA and WAA, and PDIV recorded at that instance was 1071Vp-p. The time domain result captured by the HHFA, as can be seen from Fig. 13a, has a slightly higher amplitude than that by the WAA. It can also be observed from the frequency spectrum shown in Fig. 13b that the HHFA is able to capture more spectral content than WAA especially in the range >800 MHz.

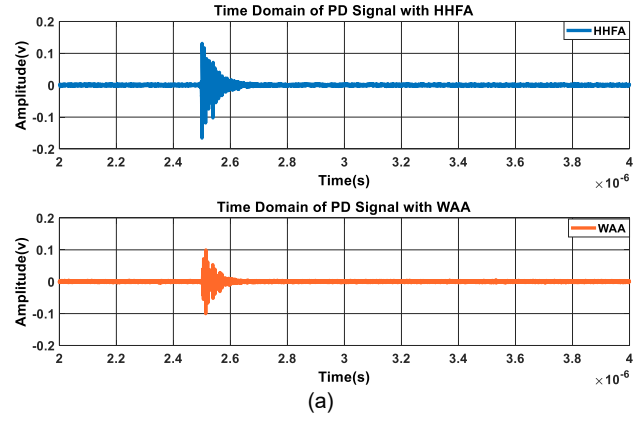


Fig. 13. Experimental measurements of PD signal with 500 MHz high pass filters. Time domain (a) and frequency domain (b) [1]

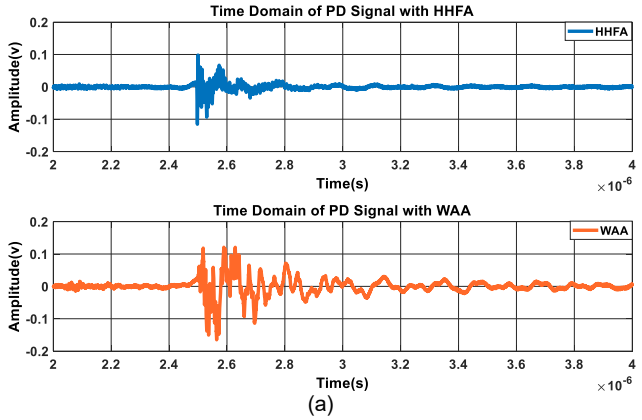


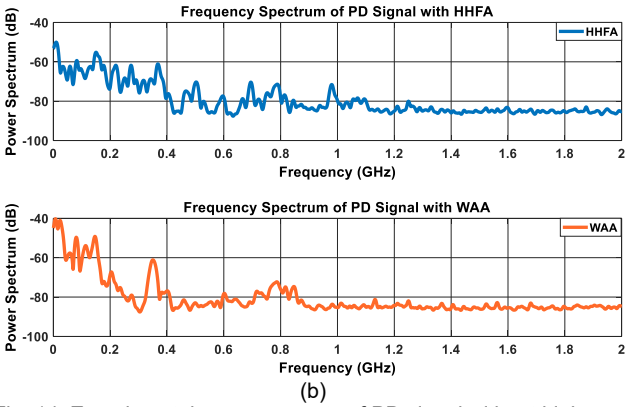


Fig. 14. Experimental measurements of PD signal without high pass filters. Time domain (a) and frequency domain (b) [1].

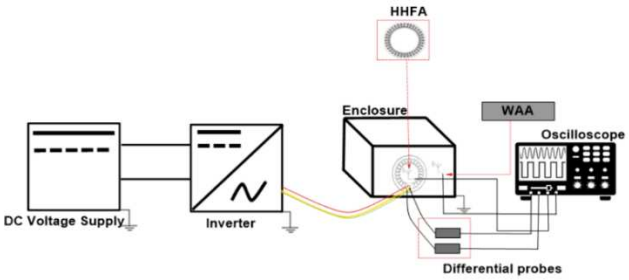


Fig. 15. Experimental setup of PD detection in inverter-fed electrical machine.

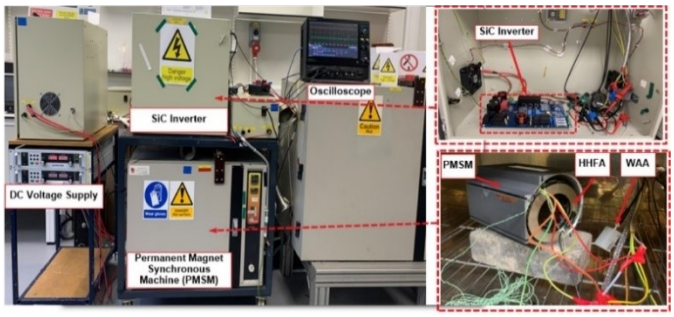


Fig. 16. Arrangement of equipment for PD detection in inverter-fed electrical machine.

This experiment was repeated without the high pass filter connected to either of the sensors. The PDIV recorded by the voltage pulse generator at this instance was 1108 Vp-p. The time domain captured PD signal in Fig.14a-b shows a comparable peak amplitude by both sensors. The WAA also appears to have significant content in the lower frequency range below 50 MHz which implies it susceptibility to capture spurious electromagnetic interference (EMI) and PWM switching noise. This also seems to confirm the relative noise immunity of the HHFA which is as a result of inherent filtering of its interstage impedance matching network topology which features a cascade of three low-pass filters and a high-pass filter.

### *C. PD Testing with Machine in Service Using Impulse Voltages*

To validate the concept proposed in [1] by physically integrating the HHFA sensor to an electrical machine in service fed by PWM inverter for online PD monitoring, the HHFA was retrofitted to the end-winding section of an aged machine. After

measuring its PDIV with the MTC2 winding analyzer, the sample was then fed with impulsive voltages from a SiC PWM-controlled inverter (Infineon IMZ120R-SIC). The schematic of the experimental setup and physical arrangement can be seen in Fig. 15 and Fig. 16, respectively.

The supplied DC voltage was set within the threshold of the measured PDIV of the sample in order to trigger PD events. The signal output of the detected PD pulse from the HHFA was connected to a 4 GHz oscilloscope sampled at 10 GS/s in accordance to the procedure outlined in [12], [53], [54] for time-domain visualization. For comparison, the WAA was positioned approximately 20 cm away from the sample in a similar setup to the experiment carried out in [45] and its output signal was also connected to another channel on the oscilloscope.

One of the challenges associated with detection of PD in inverter-fed machines is the difficulty in discriminating PD signal from noise that emanates either from WBG device switching or from external EMI. As reported in [44], [45], PD events usually occur at the voltage reversal following a commutation instant of high *dv/dt* in the so-called blind region where PD is considered very difficult to be detected. Accordingly, the traditional PD detection schemes either implement some non-trivial signal processing techniques or use an external high-pass filters to subjectively reject some predetermined cut-off frequencies. Experiments summarized here are intended to demonstrate the benefits of the proposed design in discriminating the PD signal of interest from other high frequency noises.

The results obtained following series of PD events are shown in Figs. 17-18, where the signals captured with both the proposed HHFA and the off-the-shelf WAA are presented. The applied inverter phase-to-ground voltages, measured with respect to the middle point of the DC link are also shown. Figs. 17(a)-18(a) show the signals in blue captured by the PD sensors directly fed to the oscilloscope. The filtered signals by a high-pass filter with 500 MHz bandwidth are shown in Fig. 18(b). As it is evident in Fig. 17, each switching event produces a ringing noise in the sensors, which may be followed by occasional additional ringing in case a PD event is produced. Due to the stochastic nature of PD, the frequency of occurrence of PD events is not constant.

As can be seen comparing Figs. 17 and 18, both the time domain signals, and the spectral content obtained with HHFA have higher intensity than the WAA, showing its superior performance in capturing high frequency signals due to the HHFA's closer proximity to the PD site. Additionally, the HHFA can discriminate PD pulses from commutation noise as shown in Fig. 17 without any additional hardware filtering and with simple threshold detection. On the other end, with the off-the-shelf WAA, the PD pulses are completely obscured by inverter commutation in Fig. 18(a). With the off-the-shelf antenna, in order to discriminate PD events in the presence of additional high frequency noise, an additional hardware filtering stage is necessary. Fig. 18(b) shows the antenna signal filtered with the 500 MHz high pass filter, demonstrating that the filter is necessary to reject the commutation noise.

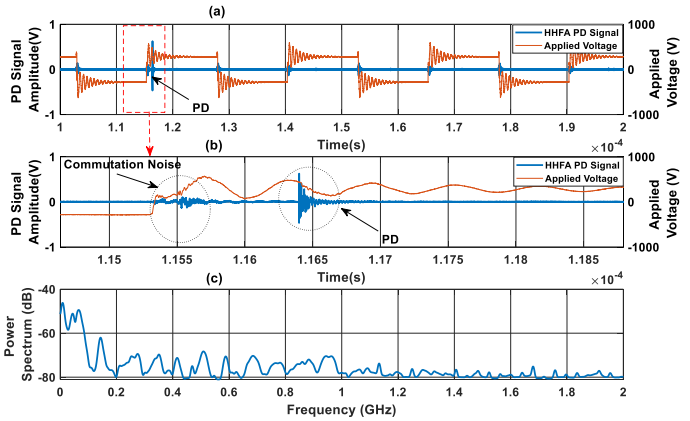


Fig. 17. Experimental measurements of PD signal from motor sample with HHFA sensor, without additional filtering. Time domain (top and zoomed-in in the middle) and frequency domain (bottom)

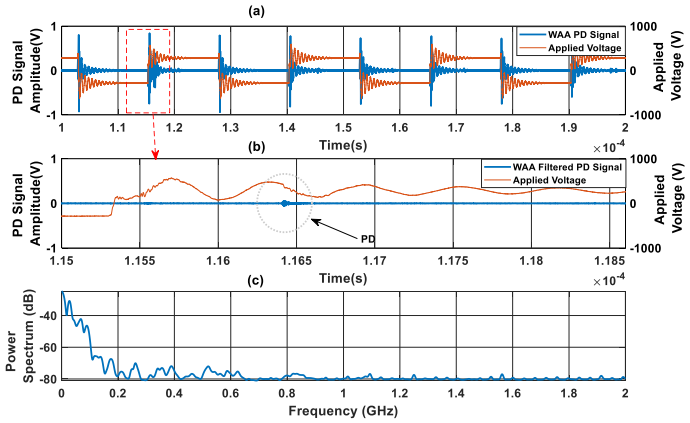


Fig. 18. Experimental measurements of PD signal from motor sample with WAA sensor. Time domain without filtering(top), zoomed-in time domain with filtering (middle) and frequency domain (bottom)

In conclusion, with its simple interstage impedance matching network with reactance cancellation, the proposed sensor is capable of identifying and discriminating the PD pulses from commutation disturbance in the blind region, demonstrating its superiority to other off-the-shelf solutions which may require additional hardware filtering and/or complex signal processing. It is also worth highlighting that, in practical applications, RF signals cannot easily propagate through metallic enclosures and screened cables (not considered in these experiments), further reducing the ability of externally mounted sensors to monitor PD activity inside the machine in most practical applications.

## IV. Conclusion

A novel low-cost and non-invasive hybrid Hilbert fractal antenna has been presented for detection of partial discharge in electrical machine insulation systems. The design, based on a dual 36-element Hilbert fractal structures which are spaced apart by 10 degrees and configured as a dipole, has a bandwidth that covers the UHF spectrum with measurement showing multiple resonance peaks in the 0.3-1.5 GHz range. Thanks to the impedance matching network, the sensor has inherent filtering capability to discriminate between commutation noise and PD pulses in the blind region where PD detection is considered impossible.

The sensor's ring shape, which facilitates its integration to the end winding of a machine, ensures its proximity to the site

of PD events, thus improving the effectiveness of detection and appropriate diagnosis. The performance and effectiveness of the sensor have been experimentally validated on a live inverter-fed electrical machine. The novel design, therefore, provides a non-invasive solution that can be retrofitted in existing machines or easily embedded at assembly stage, providing an effective and low-cost solution for condition monitoring in reliability critical applications.

## ACKNOWLEDGMENT

The authors acknowledge the Nigerian Petroleum Training and Development Fund (PTDF) for supporting this work as well as the Engineering and Physical Research Council EPSRC, under grant EP/S00081X/1, and the European Commission under Clean Sky Programme, grant 101008082. For the purpose of open access, the authors have applied a Creative Commons Attribution (CC BY) licence to any Author Accepted Manuscript version arising.

## REFERENCES

[1] Y. L. Ogundiran, A. Griffo, S. Sundeep, F. A. Gonzalez, and J. Wang, "A Novel Ring-Shaped Fractal Antenna for Partial Discharge Detection," in *2021 IEEE Energy Conversion Congress and Exposition (ECCE)*, 2021, pp. 5111–5117, doi: 10.1109/ecce47101.2021.9595017.

[2] J. C. G. Wheeler, "Effects of converter pulses on the electrical insulation in low and medium voltage motors," *IEEE Electr. Insul. Mag.*, vol. 21, no. 2, pp. 22–29, Mar. 2005, doi: 10.1109/MEI.2005.1412216.

[3] D. Bogh, S. Member, J. Coffee, G. Stone, and J. Custodio, "Partial-Discharge-Inception Testing on Low-Voltage Motors," vol. 42, no. 1, pp. 148–154, 2006.

[4] J. Millan, P. Godignon, X. Perpina, A. Perez-Tomas, and J. Rebollo, "A survey of wide bandgap power semiconductor devices," *IEEE Trans. Power Electron.*, vol. 29, no. 5, pp. 2155–2163, 2014, doi: 10.1109/TPEL.2013.2268900.

[5] J. Biela, M. Schweizer, S. Waffler, and J. W. Kolar, "SiC versus Si—Evaluation of Potentials for Performance Improvement of Inverter and DC–DC Converter Systems by SiC Power Semiconductors," *IEEE Trans. Ind. Electron.*, vol. 58, no. 7, pp. 2872–2882, 2011, doi: 10.1109/TIE.2010.2072896.

[6] A. Elasser and T. P. Chow, "Silicon carbide benefits and advantages for power electronics circuits and systems," *Proc. IEEE*, vol. 90, no. 6, pp. 969–986, 2002, doi: 10.1109/JPROC.2002.1021562.

[7] L. Fu, X. Zhang, M. Scott, C. Yao, and J. Wang, "The evaluation and application of wide bandgap power devices," in *2014 IEEE Conference and Expo Transportation Electrification Asia-Pacific (ITEC Asia-Pacific)*, 2014, pp. 1–5, doi: 10.1109/ITEC-AP.2014.6941195.

[8] H. Qin, B. Zhao, X. Nie, J. Wen, and Y. Yan, "Overview of SiC power devices and its applications in power electronic converters," in *2013 IEEE 8th Conference on Industrial Electronics and Applications (ICIEA)*, 2013, pp. 466–471, doi: 10.1109/ICIEA.2013.6566414.

[9] S. Sundeep, J. B. Wang, A. Griffo, and F. Alvarez-Gonzalez, "Anti-resonance Phenomenon and Peak Voltage Stress within PWM Inverter Fed Stator Winding," *IEEE Trans. Ind. Electron.*, vol. 0046, no. c, 2021, doi: 10.1109/TIE.2020.3048286.

[10] S. Sundeep, J. Wang, and A. Griffo, "Prediction of Transient Voltage Distribution in Inverter-fed Stator Winding, Considering Mutual Couplings in Time Domain," 2020, doi: 10.1109/ECCE44975.2020.9235981.

[11] IEC 60034-18-42 - TS Ed. 1.0, "Rotating Electrical Machines - Part 18-42: Qualification and Type Tests for Type II-Electrical Insulation Systems Used in Rotating Electrical Machines Fed from Voltage Converters," *TS*, vol. 60, pp. 18–34, 2008.

[12] IEC 60034-18-41- TS Ed. 1.0, "Part 18-41: Partial discharge free electrical insulation systems (Type I) used in rotating electrical machines fed from voltage converters – Qualification and quality control tests," no. Type I, 2015.

[13] M. Tozzi, A. Cavallini, and G. C. Montanari, "Monitoring off-line and on-line PD under impulsive voltage on induction motors - Part 2: Testing," *IEEE Electr. Insul. Mag.*, vol. 27, no. 1, pp. 14–21, 2011, doi: 10.1109/MEI.2011.5699443.

[14] W. Yin, "Failure mechanism of winding insulations in inverter-fed motors," *IEEE Electr. Insul. Mag.*, vol. 13, no. 6, pp. 18–23, 1997, doi: 10.1109/57.637150.

[15] M. Tozzi, A. Cavallini, and G. C. Montanari, "Monitoring off-line and on-line PD under impulsive voltage on induction motors - Part 1: Standard procedure," *IEEE Electr. Insul. Mag.*, vol. 26, no. 4, pp. 16–26, 2010, doi: 10.1109/MEI.2010.5511185.

[16] I. Culbert, B. Lloyd, and G. Stone, "Stator insulation problems caused by variable speed drives," *PCIC Eur. 2009 - 6th Pet. Chem. Ind. Conf. Eur. - Electr. Instrum. Appl.*, pp. 187–192, 2009.

[17] F. Alvarez-Gonzalez, D. Hewitt, A. Griffo, J. Wang, M. Diab, and X. Yuan, "Design of Experiments for Stator Windings Insulation Degradation under High dv/dt and High Switching Frequency," *ECCE 2020 - IEEE Energy Convers. Congr. Expo.*, no. 978, pp. 789–795, 2020, doi: 10.1109/ECCE44975.2020.9235940.

[18] L. Lusuardi, A. Rumi, A. Cavallini, D. Barater, and S. Nuzzo, "Partial Discharge Phenomena in Electrical Machines for the More Electrical Aircraft. Part II: Impact of Reduced Pressures and Wide Bandgap Devices," *IEEE Access*, vol. 9, pp. 27485–27495, 2021, doi: 10.1109/ACCESS.2021.3058089.

[19] A. Cavallini, D. Fabiani, and G. C. Montanari, "Power electronics and electrical insulation systems - Part 2: Life modeling for insulation design," *IEEE Electr. Insul. Mag.*, vol. 26, no. 4, pp. 33–39, 2010, doi: 10.1109/MEI.2010.5511187.

[20] R. Bartnikas, "Partial discharges. Their mechanism, detection and measurement," *IEEE Trans. Dielectr. Electr. Insul.*, vol. 9, no. 5, pp. 1–10, 2002.

[21] G. C. Stone, "Condition monitoring and diagnostics of motor and stator windings - A review," *IEEE Trans. Dielectr. Electr. Insul.*, vol. 20, no. 6, pp. 2073–2080, 2013, doi: 10.1109/TDEI.2013.6678855.

[22] M. Tozzi, A. Cavallini, and G. C. Montanari, "Monitoring off-line and on-line PD Under Impulsive Voltage on Induction - Part 3: Criticality*," *Test*, pp. 26–33, 2010.

[23] D. Fabiani, A. Cavallini, and G. C. Montanari, "A UHF technique for advanced PD measurements on inverter-fed motors," *IEEE Trans. Power Electron.*, vol. 23, no. 5, pp. 2546–2556, 2008, doi: 10.1109/TPEL.2008.2002069.

[24] T. Billard, T. Lebey, and F. Fresnet, "Partial discharge in electric motor fed by a PWM inverter: Off-line and on-line detection," *IEEE Trans. Dielectr. Electr. Insul.*, vol. 21, no. 3, pp. 1235–1242, 2014, doi: 10.1109/TDEI.2014.6832270.

[25] W. Zhou, P. Wang, Z. Zhao, Q. Wu, and A. Cavallini, "Design of an Archimedes spiral antenna for PD tests under repetitive impulsive voltages with fast rise times," *IEEE Trans. Dielectr. Electr. Insul.*, vol. 26, no. 2, pp. 423–430, 2019, doi: 10.1109/TDEI.2018.007738.

[26] P. Wang, S. Ma, S. Akram, K. Zhou, Y. Chen, and M. T. Nazir, "Design of Archimedes Spiral Antenna to Optimize for Partial Discharge Detection of Inverter Fed Motor Insulation," *IEEE Access*, vol. 8, pp. 193202–193213, 2020, doi: 10.1109/ACCESS.2020.3033300.

[27] S. Park, K. Jung, and S. Member, "Design of a Circularly-Polarized UHF Antenna for Partial Discharge Detection," vol. 8, 2020, doi: 10.1109/ACCESS.2020.2991158.

[28] J. Li, P. Wang, T. Jiang, L. Bao, and Z. He, "UHF stacked hilbert antenna array for partial discharge detection," *IEEE Trans. Antennas Propag.*, vol. 61, no. 11, pp. 5798–5801, 2013, doi: 10.1109/TAP.2013.2276453.

[29] A. A. Zahed, A. H. El-Hag, N. Qaddoumi, R. Hussein, and K. B. Shaban, "Comparison of different fourth order Hilbert fractal antennas for partial discharge measurement," *IEEE Trans. Dielectr. Electr. Insul.*, vol. 24, no. 1, pp. 175–182, 2017, doi: 10.1109/TDEI.2016.005862.

[30] F. Ashari and U. Khayam, "Design and fabrication of vivaldi antenna as partial discharge sensor," 2018, doi: 10.1109/ICEVT.2017.8323537.

[31] K. Nakamura, T. Uchimura, and M. Kozako, "Comparison of Sensor Detection Sensitivity in Repetitive Partial Discharge Inception Voltage Measurement for Twisted Pair Placed in Stator," pp. 239–242, 2016.

[32] T. Kubo *et al.*, "Sensitivity characteristics of partial discharge electromagnetic sensor located in stator core," *Proc. Int. Symp. Electr. Insul. Mater.*, vol. 2, pp. 680–683, 2017, doi: 10.23919/ISEIM.2017.8166582.

[33] A. Cavallini, G. C. Montanari, and A. Salsi, "Characterization of patch antennae for PD detection in power cables," 2007, doi: 10.1109/CEIDP.2007.4451565.

[34] E. P. T. Kerja, “Partial Discharge Inception Voltage of Twisted Pair Samples under Long-Time Repetitive Bipolar Impulses,” *Angew. Chemie Int. Ed. 6(11), 951–952.*, vol. 13, no. April, pp. 15–38, 2004.
[35] K. Kimura, S. Ushirone, T. Koyanagi, Y. Iiyama, S. Ohtsuka, and M. Hikita, “Study of PD behaviors on a crossed sample of magnet-wire with repetitive bipolar impulses for inverter-fed motor coil insulation,” *Annu. Rep. - Conf. Electr. Insul. Dielectr. Phenomena, CEIDP*, vol. 2005, pp. 393–396, 2005, doi: 10.1109/CEIDP.2005.1560703.
[36] K. Kimura, S. Ushirone, T. Koyanagi, Y. Iiyama, S. Ohtsuka, and M. Hikita, “Fluctuation of partial discharge inception voltage and discharge location of twisted pair sample under repetitive impulse voltage,” 2005, doi: 10.1109/iseim.2005.193365.
[37] G. C. Stone and V. Warren, “Objective methods to interpret partial-discharge data on rotating-machine stator windings,” *IEEE Transactions on Industry Applications*. 2006, doi: 10.1109/TIA.2005.861273.
[38] IEEE Standards Association, *1434-2012 IEEE guide for the measurement of partial discharges in AC electric machinery*, vol. 2014. 2012.
[39] T. Billard, T. Lebey, P. Castelan, and Y. Deville, “Partial discharge monitoring in twisted pair using non-intrusive sensors: Numerical analysis,” 2013, doi: 10.1109/CEIDP.2013.6748213.
[40] G. C. et all Stone, “Electrical Insulation for Rotating Machines: Design, Evaluation, Aging, Testing, and Repair,” *IEEE Press Ser. Power Eng.*, vol. 1, no. 4, p. 638, 2014.
[41] IEC 61934 TS Ed. 1.0, “Electrical Measurements of Partial Discharges During Short Risetime Repetitive Voltage Impulses,” *Electrical Measurements of Partial Discharges During Short Risetime Repetitive Voltage Impulses*. 2006.
[42] G. Robles, M. Sanchez-Fernandez, R. Albarracin Sanchez, M. V. Rojas-Moreno, E. Rajo-Iglesias, and J. M. Martinez-Tarifa, “Antenna parametrization for the detection of partial discharges,” *IEEE Trans. Instrum. Meas.*, vol. 62, no. 5, pp. 932–941, 2013, doi: 10.1109/TIM.2012.2223332.
[43] M. Tozzi, “Partial Discharges in Power Distribution Electrical Systems : Pulse Propagation Models and Detection Optimization,” *Univ. Bol. - PhD Thesis*, 2010.
[44] E. Lindell, T. Bengtsson, J. Blennow, and S. M. Gubanski, “Measurement of partial discharges at rapidly changing voltages,” *IEEE Trans. Dielectr. Electr. Insul.*, vol. 15, no. 3, pp. 823–831, 2008, doi: 10.1109/TDEI.2008.4543120.
[45] R. Ghosh, P. Seri, R. Hebner, and G. C. Montanari, “Noise Rejection and Detection of Partial Discharges under Repetitive Impulse Supply Voltage,” *IEEE Trans. Ind. Electron.*, vol. 0046, no. c, pp. 1–1, 2019, doi: 10.1109/tie.2019.2921281.
[46] L. J. Chu, “Physical limitations of omni-directional antennas,” *J. Appl. Phys.*, 1948, doi: 10.1063/1.1715038.
[47] H. A. Wheeler, “Fundamental limitations of small antennas,” *Proc. IRE*, 1947, doi: 10.1109/JRPROC.1947.226199.
[48] C. A. Balanis, *Antenna Design, Analysis and Design*, 4th ed. Hoboken, New Jersey: John Wiley & Sons, 2016.
[49] D. H. Werner and R. Mittra, *Frontiers in electromagnetics*. 1999.
[50] D. M. Pozar, *Microwave Engineering, 4th Edition*. 2012.
[51] Z. N. Chen, D. Liu, H. Nakano, X. Qing, and T. Zwick, *Handbook of antenna technologies*. 2016.
[52] C. Poole and I. Darwazeh, *Microwave Active Circuit Analysis and Design*. 2015.
[53] IEEE Standards Association, *IEEE guide for the measurement of partial discharges in AC electric machinery*, vol. 2014. 2012.
[54] B. Standard, “IEC 60270 : partial discharge measurements,” *Br. Stand.*, 2001, [Online]. Available: http://cds.cern.ch/record/840339.